

HYDRODYNAMICS OF BINARY COALESCENCE

Frederic A. Rasio

Institute for Advanced Study, Olden Lane, Princeton, NJ 08540, USA

ABSTRACT. Hydrostatic equilibrium configurations for close binary systems can become *globally unstable*. Instabilities arise from the strong tidal interaction between the two components, which tends to make the effective two-body potential steeper than $1/r$. As a result, a circular orbit can become unstable to small radial perturbations. The instability can be either secular or dynamical. In both cases it leads to the coalescence and merging of the two components on a time scale much shorter than the typical lifetime of a stable system. In a secularly unstable system, orbital decay is driven by viscous dissipation and proceeds on a time scale comparable to the synchronization time of a stable binary. In a dynamically unstable system, the two stars suddenly plunge toward each other and merge hydrodynamically in just a few orbital periods.

Introduction

The coalescence and merging of two stars into a single object is the almost inevitable endpoint of close binary evolution. Loss of angular momentum through a variety of dissipation mechanisms always leads to orbital decay. It was only recently realized that the late stages of this orbital decay can often become hydrodynamic in nature, with the final merging of the two stars occurring on a time scale much shorter than the angular-momentum loss time scale (Rasio & Shapiro 1992, 1994, hereafter RS; Lai, Rasio, & Shapiro 1993a,b, 1994,a,b, hereafter LRS). This is because *global instabilities* can drive the binary system to rapid coalescence once the tidal interaction between the two components becomes sufficiently strong. When the binary system becomes unstable, rapid orbital decay is inevitable, even in the absence of an effective angular-momentum loss mechanism. This orbital decay of unstable systems can be either *dynamical*, with the two stars coalescing in just a few orbital periods, or *secular*, i.e., driven by internal viscous dissipation in the fluid. In this latter case, the orbit decays by continuously transferring angular momentum to an internal shear flow, while the system attempts unsuccessfully to maintain uniform fluid rotation.

Binary coalescence has been associated with a number of astrophysical phenomena of great current interest. Close neutron-star binaries are most important sources of gravitational radiation in the Universe, and are the primary targets for the LIGO project (Abramovici et al. 1992). The coalescence of two neutron stars is at the basis of numerous models of γ -ray bursters (see Narayan, Paczyński, & Piran 1992 and references therein; Colpi & Rasio, these Proceedings). Double white-dwarf systems are now generally thought to be the progenitors of Type Ia supernovae (Iben & Tutukov 1984; Yungelson et al. 1994). They are also promising sources of low-frequency gravitational waves that should be easily detectable by future space-based interferometers (Evans, Iben, & Smarr 1987). In addition to producing supernovae, the coalescence of two white dwarfs may also lead in certain cases to the formation by gravitational collapse of an isolated millisecond pulsar (Chen & Leonard 1993) or the formation of blue subdwarf stars in globular clusters (Bailyn 1993). In the case of coalescing magnetized white dwarfs, a neutron star with extremely high magnetic field may form, and such an object has also been proposed as a source of γ -ray bursts (Usov 1992). Coalescing main-sequence star binaries are likely progenitors for the numerous blue stragglers found in stellar clusters (Mateo et al. 1990), and are observed directly as Algol and W UMa systems (Rucinski 1992, and these Proceedings).

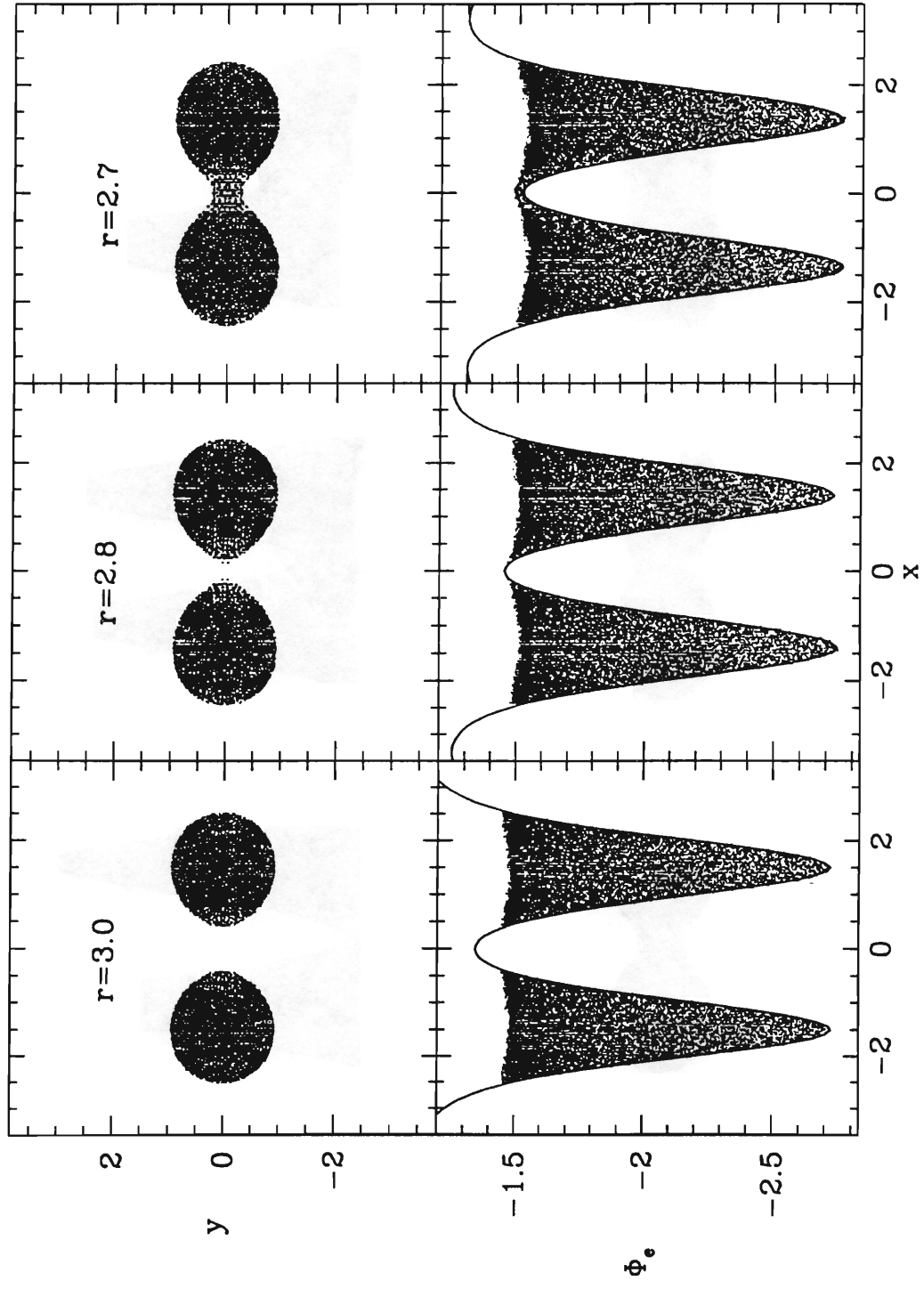
Dynamical Instabilities

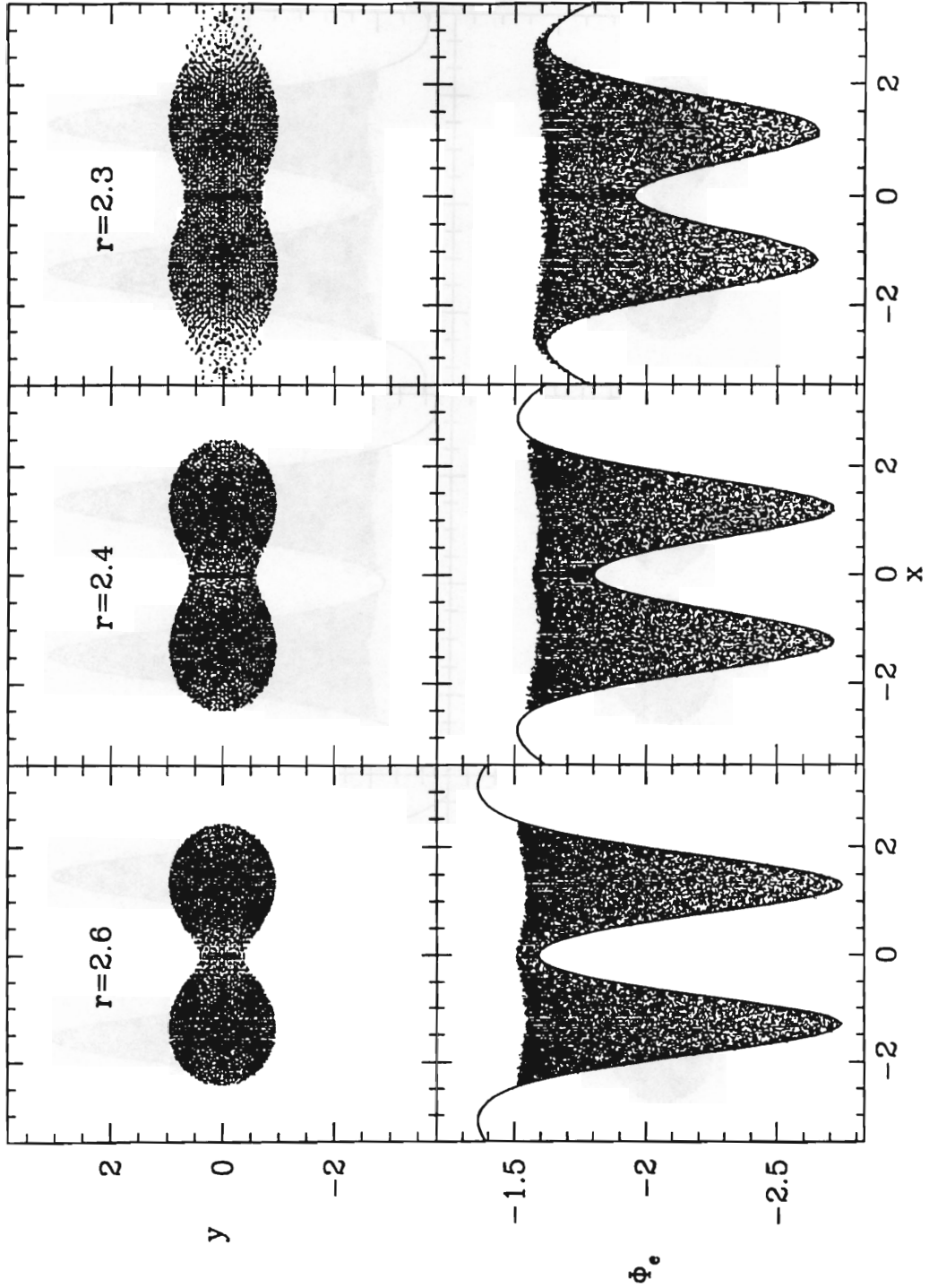
When the two components of a binary system are sufficiently close, the strong tidal interaction can make the effective two-body potential governing the orbital motion deviate quite significantly from a Keplerian $1/r$ potential. Since the effective potential becomes *steeper* than $1/r$, a circular orbit can become *dynamically unstable* (see, e.g., Goldstein 1980, Chap. 2), just like general relativity can make circular orbits become unstable sufficiently close to a black hole (see, e.g., Shapiro & Teukolsky 1983, §12.4). The existence of this dynamical instability in close binary configurations containing an *incompressible fluid* has been known for a long time (Chandrasekhar 1969, 1975; Tassoul 1975). The recent work of RS and LRS shows that it extends quite far into the compressible regime, so that it can affect real stars made of compressible fluid. Self-gravity is of course essential here, and the usual Roche model (which treats close binaries as made of massless gas in the effective potential of two point masses) cannot be used. Instead, three-dimensional hydrodynamics must be used, which until very recently was beyond the capabilities of most computers.

For an incompressible fluid, the onset of instability corresponds to a binary configuration which is still slightly detached (Tassoul 1975). The same is true for binary neutron stars with stiff equations of state (RS). However, for most normal stars with centrally concentrated mass profiles, significant deviations from Keplerian behavior occur only when the outer layers of the two stars are overlapping, i.e., for contact configurations. As an example, consider a sequence of equilibrium binary configurations for two identical polytropes with $\Gamma = 5/3$ (Fig. 1). These could be simple models for two low-mass white dwarfs or main-sequence stars (although in reality these systems are unlikely to have a mass ratio close to unity; similar polytropic configurations with higher values of Γ have been considered by RS for modeling neutron star binaries, where the observed mass ratios are very close to 1). The dynamical stability of these equilibrium models can be tested directly by integrating numerically on a supercomputer the hydrodynamical equations in three dimensions. The results of such integrations, using the smoothed particle hydrodynamics (SPH) method (see Monaghan 1992 for a recent review), are shown in Figures 2-4.

As predicted by the linear perturbation calculations of LRS, binary systems with sufficiently close components are found to be dynamically unstable (Fig. 2). Numerically, one can continue the integrations well into the nonlinear regime and determine the final (stable) equilibrium configuration of the merger product (Figs. 3 and 4). It is tempting to envision (cf. Rasio 1993) that the secular evolution of a contact main-sequence star binary through loss of angular momentum (by gravitational radiation or via magnetized winds), possibly accelerated by viscous dissipation (see below), could bring the two components sufficiently close together to make the system unstable. The object depicted in Figure 4 could then be a young blue straggler. For two white dwarfs, the merger product may well be above the Chandrasekhar mass, and should therefore explode as a (Type Ia) supernova, or perhaps collapse to a neutron star. The rapid rotation (cf. Fig. 4) and possibly high mass (up to $2M_{Ch}$) of the object must be taken into account for determining its final fate. This has not been done in recent theoretical calculations (Nomoto 1987; Isern, these Proceedings), where a quasi-spherical (nonrotating) white dwarf just below the Chandrasekhar limit is assumed to accrete slowly from a disk.

Figure 1. (following two pages) Sequence of corotating binary configurations with decreasing separation r , for two identical polytropes with $\Gamma = 5/3$. Exact solutions of the hydrostatic equilibrium equation were calculated numerically in three dimensions using the smoothed particle hydrodynamics (SPH) method. On top, projections of all SPH particles into the orbital (x, y) plane are shown. At the bottom, the effective potential (exact gravitational potential of the fluid plus centrifugal potential) $\Phi_e(x, y = 0, z = 0)$ along the binary axis is shown (solid lines), together with the positions of all SPH particles in the (x, Φ_e) space. Units are such that $G = M = R = 1$, where M and R are the mass and radius of one unperturbed (spherical) star. Contact configurations are obtained for $r/R \lesssim 2.8$. Configurations with $r/R \lesssim 2.7$ are secularly unstable; they become dynamically unstable for $r/R \lesssim 2.5$. For $r/R \lesssim 2.3$, the fluid overflows through the outer Lagrangian points and hydrostatic equilibrium solutions no longer exist.





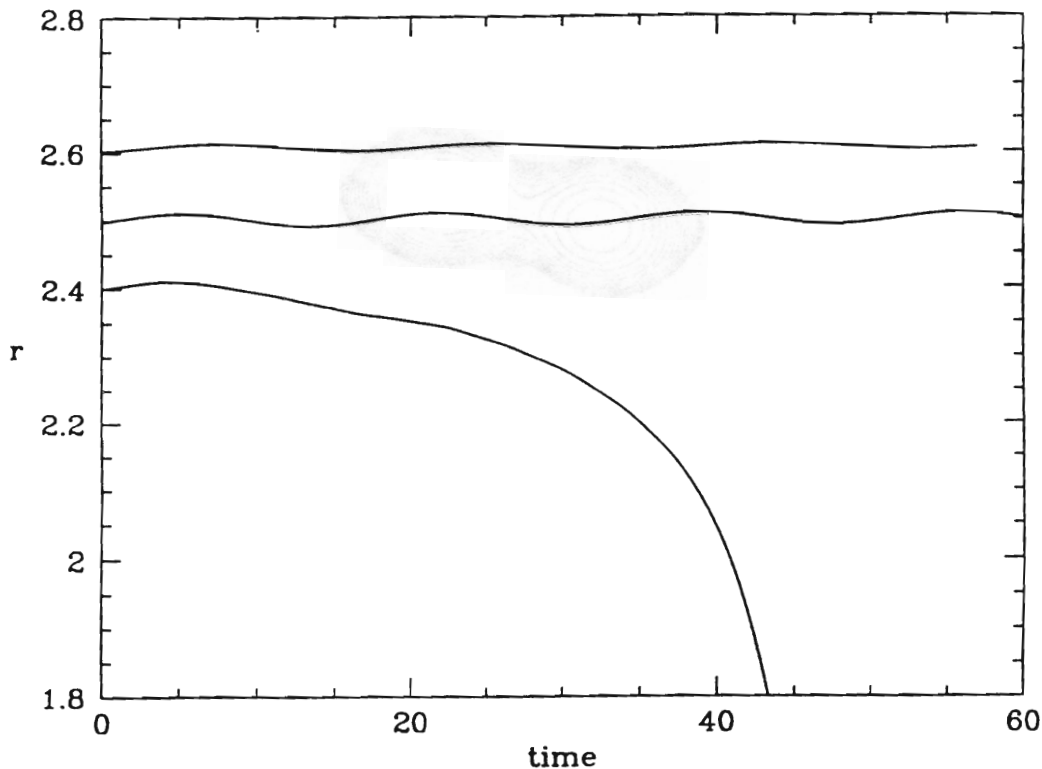
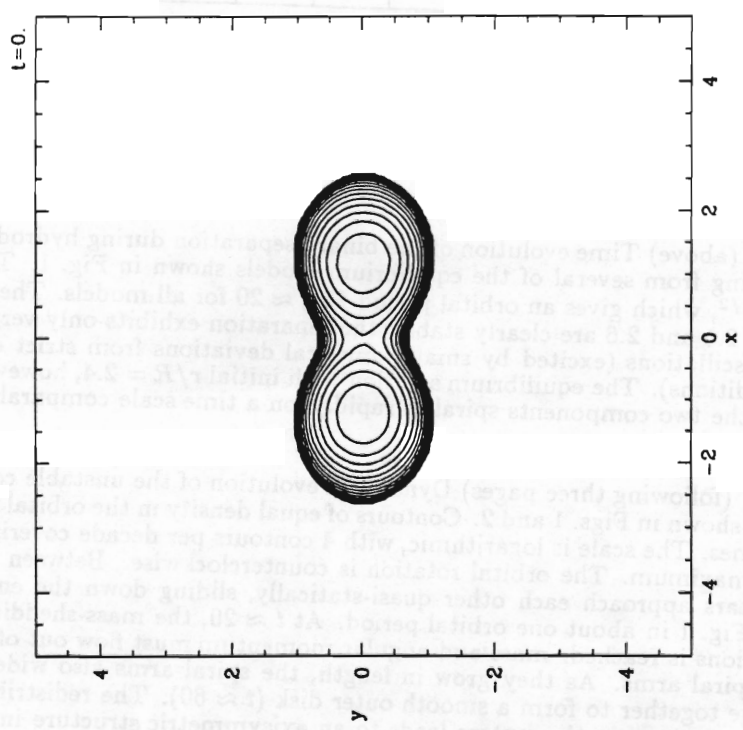
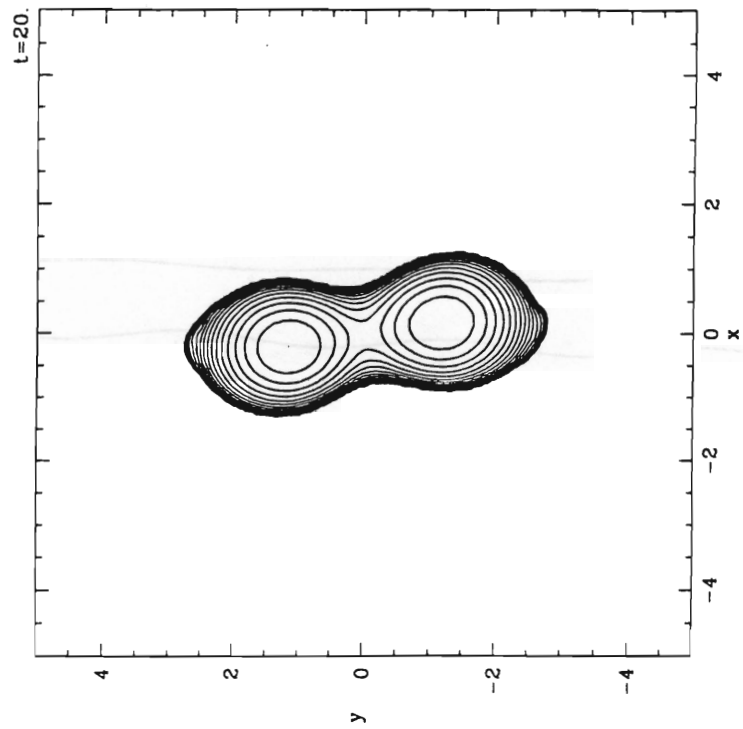
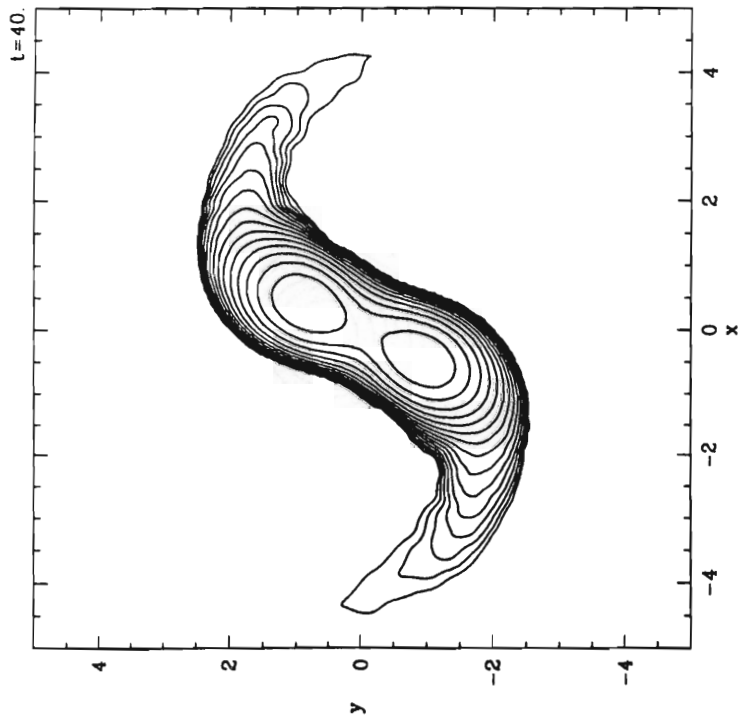
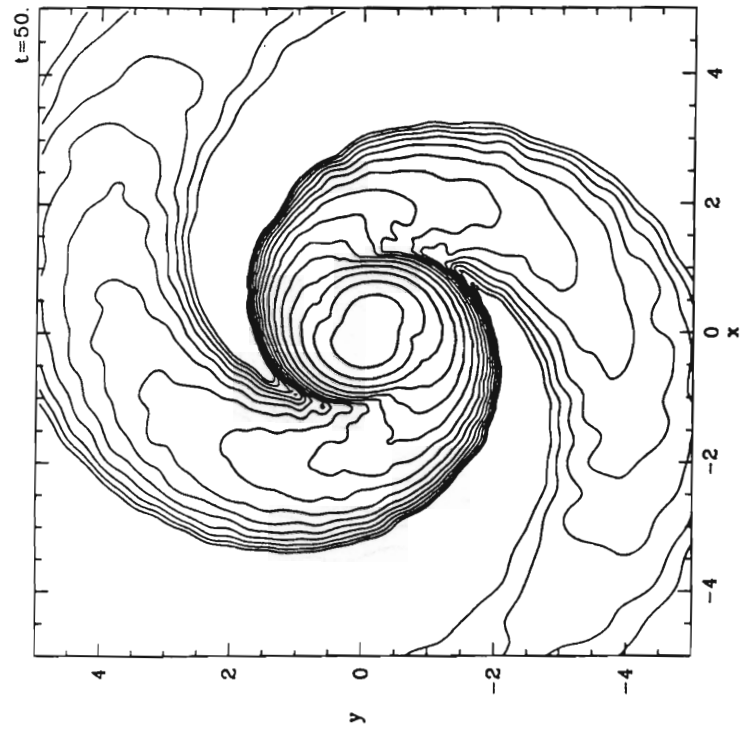
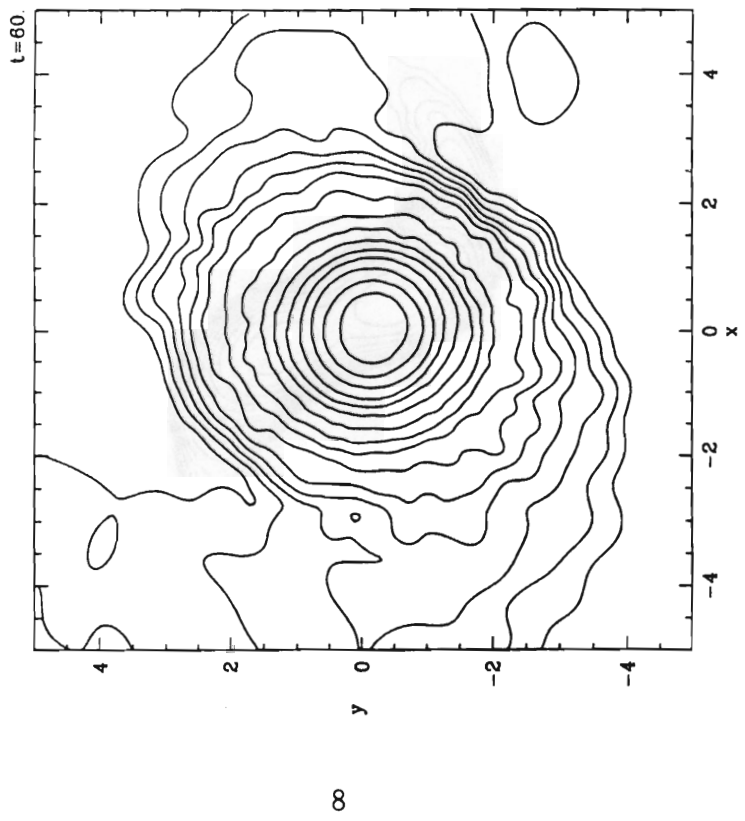
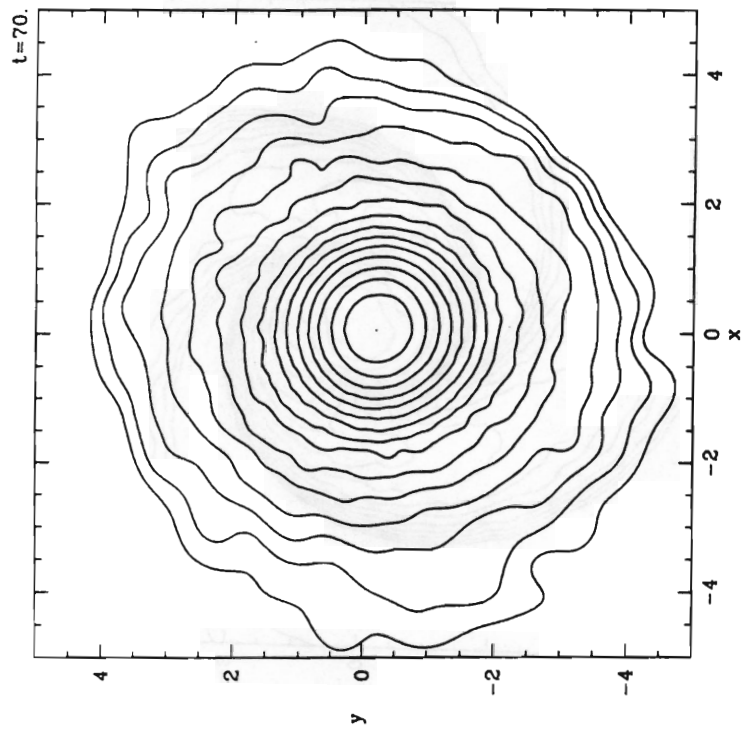


Figure 2. (above) Time evolution of the binary separation during hydrodynamical integrations starting from several of the equilibrium models shown in Fig. 1. Time is in units of $(R^3/GM)^{1/2}$, which gives an orbital period $P_{orb} \approx 20$ for all models. The binaries with initial $r/R = 2.5$ and 2.6 are clearly stable: the separation exhibits only very small-amplitude epicyclic oscillations (excited by small numerical deviations from strict equilibrium in the initial conditions). The equilibrium solution with initial $r/R = 2.4$, however, is dynamically unstable: the two components spiral in rapidly, on a time scale comparable to P_{orb} .

Figure 3. (following three pages) Dynamical evolution of the unstable contact binary with $r/R = 2.4$ shown in Figs. 1 and 2. Contours of equal density in the orbital plane are shown at various times. The scale is logarithmic, with 4 contours per decade covering 4 decades down from the maximum. The orbital rotation is counterclockwise. Between $t = 0$ and $t \approx 20$, the two stars approach each other quasi-statically, sliding down the end of the sequence shown in Fig. 1 in about one orbital period. At $t \approx 20$, the mass-shedding limit for binary configurations is reached: mass and angular momentum must flow out of the central region through spiral arms. As they grow in length, the spiral arms also widen and, eventually, they merge together to form a smooth outer disk ($t \approx 60$). The redistribution of mass and angular momentum in the system leads to an axisymmetric structure in stable hydrostatic equilibrium at the end of the calculation.







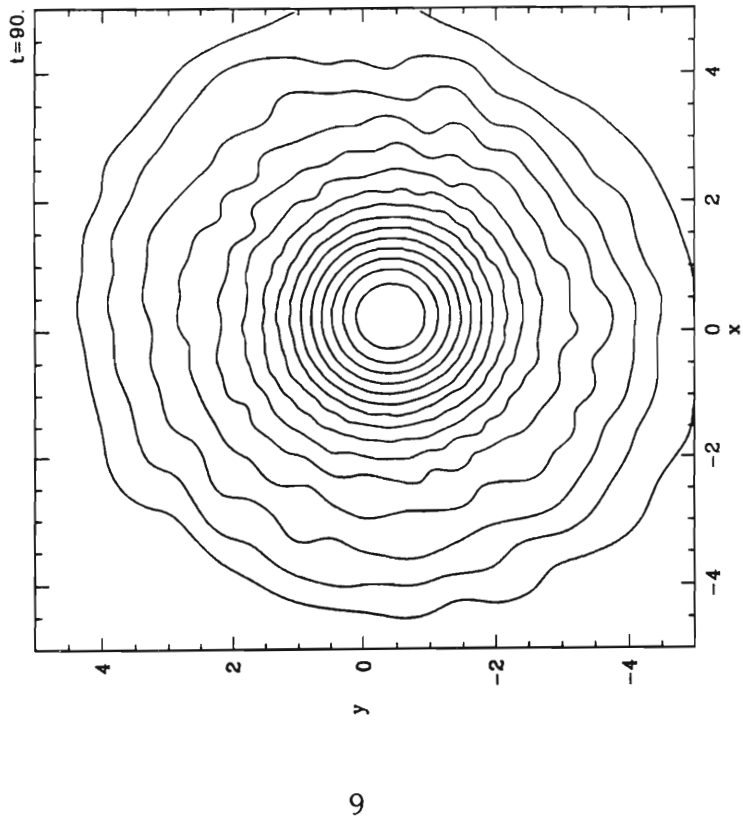
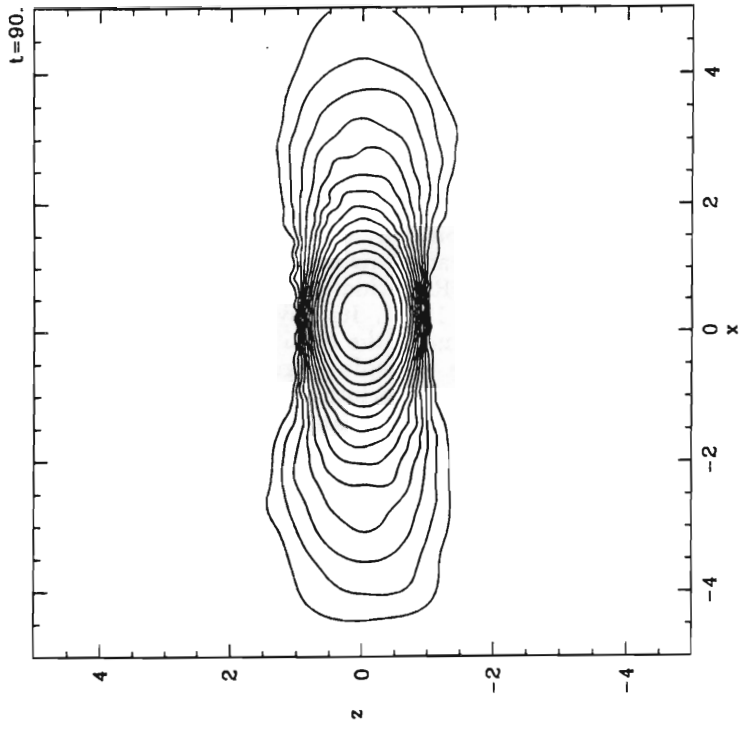


Figure 4. (previous page) Final merged configuration resulting from the dynamical evolution shown in Fig. 3. Density contours in the orbital (x, y) plane and the meridional (x, z) plane are shown. Conventions are as in Fig. 3. The object is rapidly rotating and highly flattened. The rotation is nearly uniform in the central core (containing about 80% of the mass), but very differential in the outer disk. The ratio of kinetic energy of rotation to gravitational binding energy is $T/|W| \approx 0.12$.

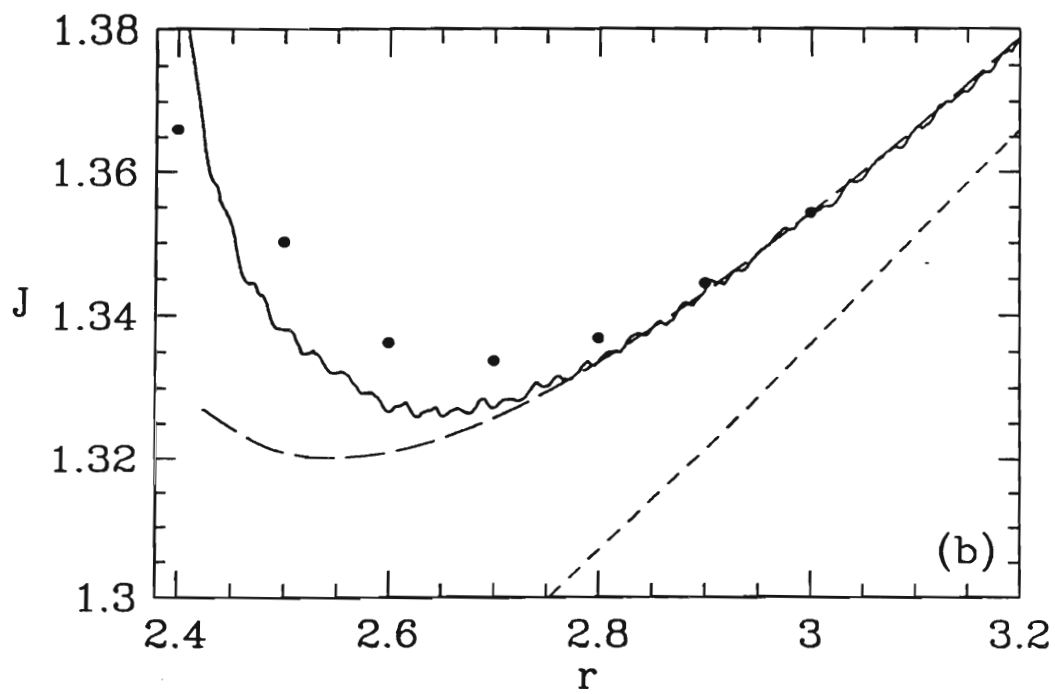
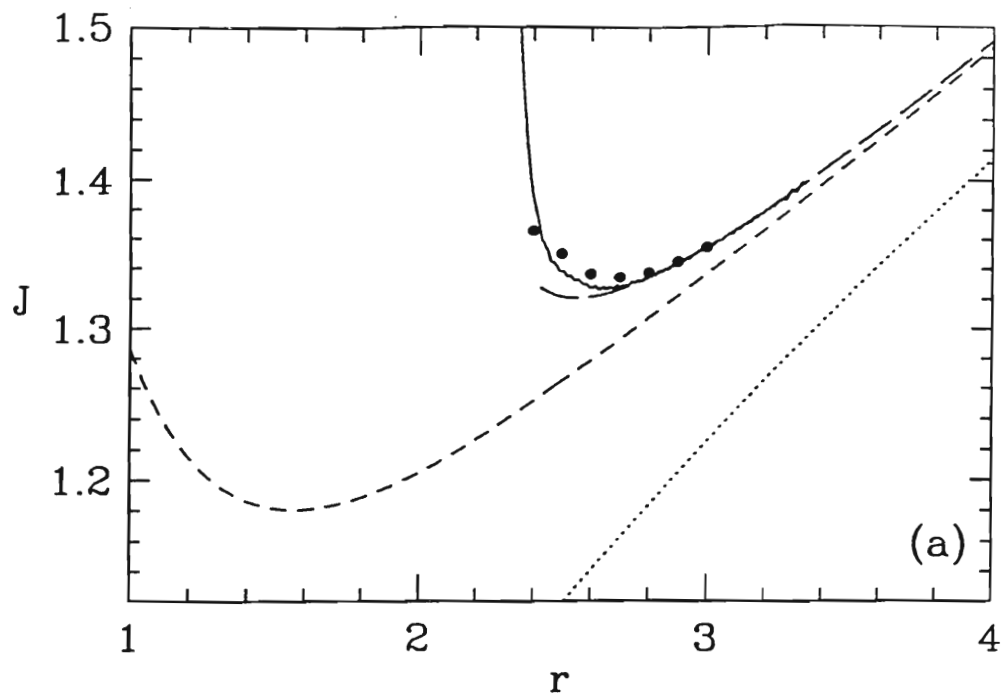
Secular Instabilities

Well before a close binary system becomes dynamically unstable (and even if it never does), another type of global instability can affect its evolution. It has been referred to by various names, such as secular instability (LRS), tidal instability (Counselman 1973; Hut 1980), and Darwin instability (Levine et al. 1993). Its physical origin is very easy to understand (Fig. 5). There exists a *minimum* value of the total angular momentum for a *synchronized* close binary. This is simply because the spin angular momentum, which *increases* as r decreases, can become comparable to the orbital angular momentum for sufficiently small r . A system that reaches the minimum of J cannot evolve further by angular momentum loss and remain synchronized. Instead, the combined action of tidal forces and viscous dissipation will drive the system *out* of synchronization and cause rapid orbital decay as angular momentum is continually transferred from the orbit to the spins.

The orbital decay of a secularly unstable binary proceeds on the (de)synchronization time scale, which is typically much shorter than the time scale associated with any angular-momentum loss mechanism (LRS). For example, for two low-mass main-sequence stars with large convective envelopes, this time scale could be as short as 10^4 yr (Zahn 1977). This may explain why the components of W UMa binaries are always observed to be in very shallow contact (Rucinski 1992): If the two components ever got closer together because of mass exchange or loss of angular momentum, the system would become secularly unstable and the two stars would quickly coalesce. The exact location of the secular stability limit (and the corresponding maximum value of the degree of contact for a stable, long-lived system) should depend sensitively on the internal structure of the binary, and, in particular, the distribution of specific entropy in the system. Thus a large sample of well-determined contact-binary parameters could be used to place interesting constraints on their internal structure.

Secular instabilities can also be important for the orbital evolution of close binaries containing a compact object in orbit around a more massive, extended star, as in high-mass X-ray binaries (Levine et al. 1993). In this case the Roche limit configuration can be secularly unstable (LRS), and it is possible that both mass transfer and orbital decay could be driven purely by internal viscous dissipation and tidal effects, rather than by stellar evolution or angular momentum loss.

Figure 5. (following page) Variation of the total angular momentum J as a function of binary separation r along the equilibrium sequence considered previously (Fig. 1). Here J is in units of $(GM^3R)^{1/2}$ and r is in units of the stellar radius R as before. The solid dots are the fully numerical results corresponding to the models of Fig. 1; the solid curves are from a simplified numerical calculation (RS). The long-dashed curves are from the quasi-analytic models of LRS, representing the stars as compressible ellipsoids; the short-dashed lines are for two rigid spheres, and the dotted line is for two point masses in a Keplerian orbit. The minimum of J at $r/R \approx 2.7$ gives the secular stability limit for synchronized configurations. In (b), a blow-up of the region around this minimum is shown. Binary systems sliding down the equilibrium $J(r)$ curve as they lose angular momentum (e.g., through gravitational radiation) must eventually attain this minimum. At that point, internal viscous dissipation will take over and drive the subsequent orbital decay on a much shorter time scale. The system can then minimize its energy (at constant angular momentum) by evolving *out* of synchronization as the orbit decays. The two stars ultimately merge, either dynamically (Fig. 3) if a dynamical instability is encountered at smaller r before the onset of mass shedding (which would be the case for the two polytropes considered here), or quasi-statically otherwise. Note that the simple two-sphere model (considered in all previous studies of the secular instability; see, e.g., Counselman 1973, Hut 1980) can give largely inaccurate results for close binaries: it predicts the minimum of J at $r/R \approx 1.6$ in this case (short-dashed line), far below the exact value determined numerically.



Acknowledgements

I thank my collaborators, Dong Lai and Stu Shapiro, for many stimulating discussions. I also acknowledge gratefully the hospitality of the ITP at UC Santa Barbara, where this manuscript was written. This work has been supported by a Hubble Fellowship, funded by NASA through Grant HF-1037.01-92A. Computations were performed on the Cornell National Supercomputer Facility.

References

- Abramovici, A., et al. 1992, *Science*, **256**, 325.
Bailyn, C. D. 1993, in *Dynamics of Globular Clusters: a Workshop in Honor of I. R. King*, eds. S. Djorgovski & G. Meylan, ASP Conf. Series, in press.
Chandrasekhar, S. 1969, *Ellipsoidal Figures of Equilibrium* (New Haven: Yale Univ. Press).
Chandrasekhar, S. 1975, *ApJ*, **202**, 809.
Chen, K., & Leonard, P. J. T. 1993, *ApJL*, **411**, L75.
Counselman, C. C. 1973, *ApJ*, **180**, 307.
Evans, C. R., Iben, I., & Smarr, L. 1987, *ApJ*, **323**, 129.
Goldstein, H. 1980, *Classical Mechanics*, 2nd ed. (Reading: Addison-Wesley).
Hut, P. 1980, *A&A*, **92**, 167.
Iben, I., & Tutukov, A. V. 1984, *ApJS*, **54**, 335.
Lai, D., Rasio, F. A., & Shapiro, S. L. 1993a, *ApJS*, **88**, 205.
Lai, D., Rasio, F. A., & Shapiro, S. L. 1993b, *ApJL*, **406**, L63.
Lai, D., Rasio, F. A., & Shapiro, S. L. 1994a, *ApJ*, in press (Jan. 10).
Lai, D., Rasio, F. A., & Shapiro, S. L. 1994b, *ApJ*, in press (April 1).
Levine, A., Rappaport, S., Deeter, J. E., Boynton, P. E., & Nagase, F. 1993, *ApJ*, **410**, 328.
Mateo, M., Harris, H. C., Nemeč, J., & Olszewski, E. W. 1990, *AJ*, **100**, 469.
Monaghan, J. J. 1992, *ARA&A*, **30**, 543.
Narayan, R., Paczyński, B., & Piran, T. 1992, *ApJL*, **395**, L83.
Nomoto, K. 1987, in *IAU Symposium 125, Origin and Evolution of Neutron Stars*, eds. D. J. Helfand & J.-H. Huang (Dordrecht: Reidel), p. 281.
Rasio, F. A. 1993, in *Proceedings of STScI Workshop on Blue Stragglers*, eds. M. Livio & R. Saffer, ASP Conf. Series, in press.
Rasio, F. A., & Shapiro, S. L. 1992, *ApJ*, **401**, 226.
Rasio, F. A., & Shapiro, S. L. 1994, *ApJ*, submitted.
Rucinski, S. M. 1992, in *The Realm of Interacting Binary Stars*, eds. J. Sahade et al. (Dordrecht: Kluwer), p. 111.
Shapiro, S. L., & Teukolsky, S. A. 1983, *Black Holes, White Dwarfs, and Neutron Stars* (New York: Wiley).
Tassoul, M. 1975, *ApJ*, **202**, 803.
Usov, V. V. 1992, *Nature*, **357**, 472.
Yungelson, L. R., Livio, M., Tutukov, A. V., & Saffer, R. A. 1994, *ApJ*, in press (Jan. 1).
Zahn, J. P. 1977, *A&A*, **57**, 383.

EXPLOSIONS OF NEUTRON STAR FRAGMENTS EJECTED DURING BINARY COALESCENCE

Monica Colpi (1) & Frederic A. Rasio (2)

(1) *Department of Physics, Università degli Studi di Milano, Milan, Italy*

(2) *Institute for Advanced Study, Princeton, NJ, USA*

ABSTRACT. Small, self-gravitating fragments of unstable neutronized matter may be produced during the final coalescence of neutron star binaries. An energy $\sim 10^{50}$ erg is expected to be released in a burst of antineutrinos and high-energy photons.

1. Introduction

It is well known that there exists a *minimum mass* M_{\min} for a neutron star, below which no stable hydrostatic equilibrium can exist. At M_{\min} , an instability to expansion is expected to be triggered by β -decays and nuclear fissions. Colpi, Shapiro, & Teukolsky (1989, 1991) have calculated the evolution of such an unstable neutron star. They showed that the star disrupts catastrophically, on a time scale of a few milliseconds to a few seconds. These calculations were carried out using realistic microphysics but an approximate dynamical model based on homogeneous Newtonian spheroids. In the first part of this paper, we summarize the results of a more recent, improved treatment (Colpi et al. 1993, hereafter CST).

The astrophysical relevance of this process has been discussed by various authors (Clark & Eardley 1977; Blinnikov et al. 1984, 1990) in the context of neutron star binaries. Early studies of the terminal evolution of these systems suggested the possibility of stable mass transfer from the lighter component to the heavier. This could result in mass stripping of the lighter neutron star down to the minimum mass. More recent investigations, however, indicate that stable mass transfer is very unlikely, except perhaps in rather special and unrealistic cases, e.g., when the mass ratio is far from unity (Bildsten & Cutler 1992; Kochanek 1992; Lai, Rasio & Shapiro 1994). In general, tidal disruption of the lighter star and coalescence of the system will occur on a dynamical time scale. In the second part of this paper, we propose a new scenario for the explosion of neutronized matter following the dynamical coalescence of two neutron stars. We discuss the possible relevance of this scenario to cosmological models of γ -ray bursters (see, e.g., Narayan, Paczyński, & Piran 1992).

2. Exploding Neutron Stars Below the Minimum Mass

CST follow the evolution of an unstable neutron star below M_{\min} using a Lagrangian hydrodynamical code that accounts for the inhomogeneous structure of the star. The seeds of the instability are the β -decaying nuclei in the crust layers. It is thus important to consider how the instability rises and spreads: Does the unstable star explode suddenly when β -decays are well under way, or does it evaporate on the β -decay time scale by slowly ejecting material from the surface? In the expansion, does a bound lower mass remnant form? To address these questions one must incorporate into the dynamical calculation a *nonequilibrium* equation of state. CST adopt the Harrison-Wheeler nuclear model, giving $M_{\min} = 0.196 M_{\odot}$. Matter consists of free electrons, dripped neutrons, and heavy nuclei unstable to β -decay. During the decompression, nuclei follow a path similar to the r -process, terminating with fission. The neutron star is initially in hydrostatic equilibrium. It is perturbed out of β -equilibrium by slowly stripping mass from its surface. The expansion is then driven by the ensuing β -decays and nuclear fissions. Stability is lost at a lower critical

mass, $M_{\text{crit}} = 0.8M_{\text{min}}$, as matter follows the nonequilibrium equation of state during the perturbation.

The evolution is found to proceed along three distinct phases: (1) In the first phase the outermost layers reach quickly the escape velocity, the outflow properties depending sensitively on the way mass stripping is numerically handled. (2) A second phase of *secular* expansion follows that involves the intermediate layers of the crust where the seeds of the instability are present. This phase, similar to an *evaporation* process, lasts $\sim 10^2$ – 10^5 s, the spread corresponding to uncertainties in the β -decay timescale and in the stripping process. (3) Following the loss of the crust layers, a phase of sudden *explosion* sets in: the inner layers accelerate abruptly, attaining escape velocity in a few milliseconds. During core explosion, nuclear transformations change the composition of matter so that it becomes progressively richer in heavy nuclei unstable to fission. The energy per baryon ϵ_B deposited by fission is ~ 0.5 – 1 MeV. A fission “wave” forms in the overlying intermediate layers that propagates inwards, heating the whole star up to a temperature $\sim 10^{10}$ K. Figure 1 illustrates the evolution during this explosive phase. The ejected debris move at a mean velocity $\sim 5 \times 10^4$ km s $^{-1}$, corresponding to a total kinetic energy output $\sim 5 \times 10^{49}$ erg. An antineutrino burst with peak luminosity $L_{\bar{\nu}} \sim 10^{50}$ – 10^{52} erg s $^{-1}$ signals the onset of the explosion.

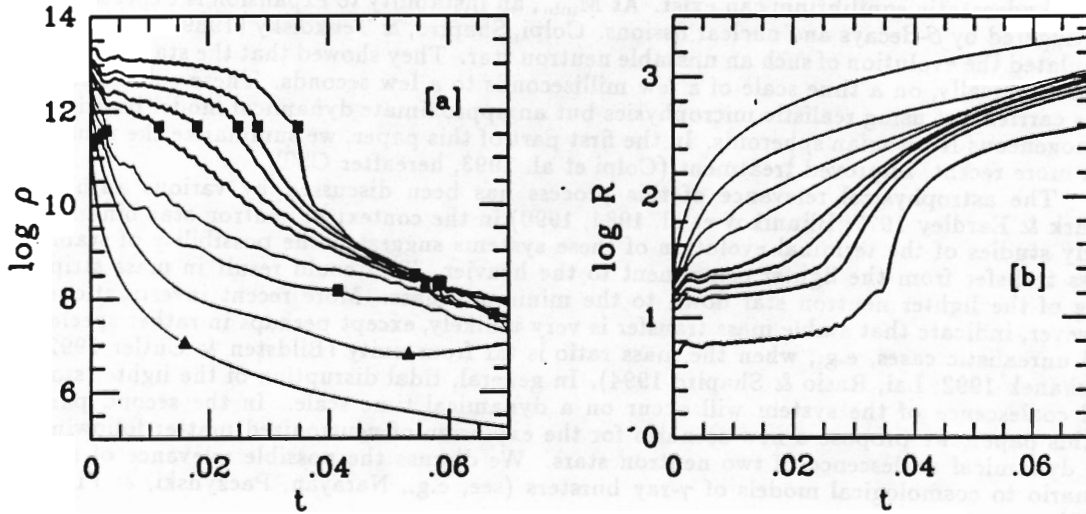


Figure 1. Density ρ in g cm $^{-3}$ [a], and radius R in km [b] as a function of time (in sec) for $M = M_{\text{crit}}$. Solid (heavy) lines denote crust (core) shells. Squares indicate the occurrence of fission; triangles, the reabsorption of dripped neutrons.

3. Explosions of Fragments Ejected During Binary Coalescence

3.1 Hydrodynamics of Neutron Star Binary Coalescence

The hydrodynamics of coalescing neutron star binaries has been studied recently by Rasio & Shapiro (1992, 1994; see also Rasio, this volume) using the smoothed particle hydrodynamics (SPH) method. When the separation between the two stars becomes smaller than a critical value $r_{\text{dyn}} \simeq 3R$, where R is the stellar radius, the system becomes *dynamically unstable* to small radial perturbations of the orbital motion (Lai et al. 1993, 1994). For neutron stars with a stiff equation of state (adiabatic exponent $\Gamma \gtrsim 2$), the onset of instability corresponds to a binary configuration that is still slightly *detached*. The instability leads to the coalescence and merging of the two stars on a time scale comparable to the orbital period. For two identical neutron stars of mass $M = 1.4 M_{\odot}$ and radius $R \simeq 10$ km, the binary separation at the onset of instability is $r_{\text{dyn}} \simeq 30$ km and the corresponding orbital period is $P_{\text{orb}} \approx 1.5$ ms. The complete dynamical coalescence and merging of the two stars into a single massive object then takes about 7 ms.

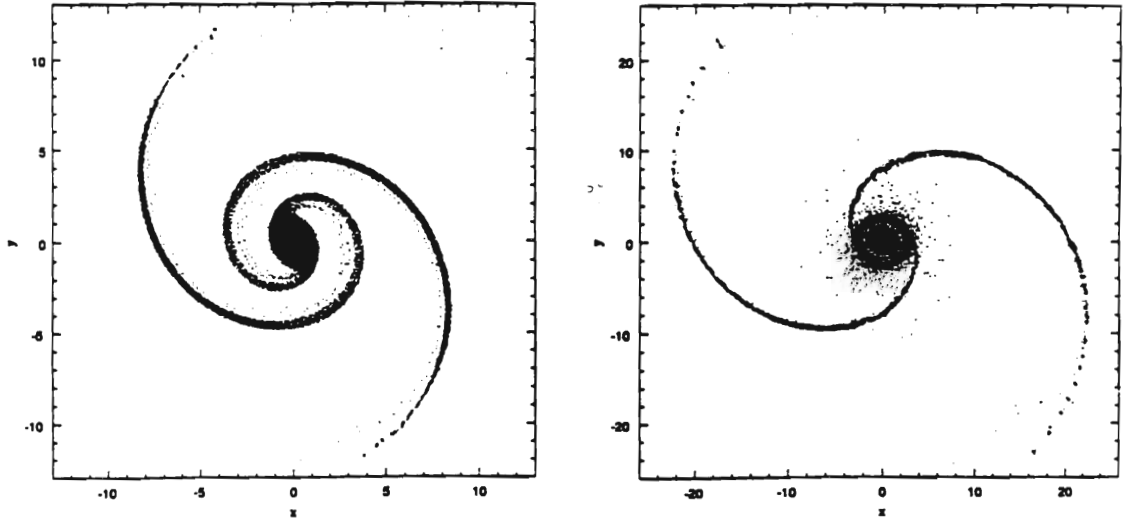


Figure 2. Rotational instabilities and mass shedding through spiral arms develop during the dynamical coalescence of two neutron stars. In this SPH calculation, two identical stars modeled as polytropes with $\Gamma = 3$ were placed initially in an equilibrium binary configuration on the verge of dynamical instability. Projections of all SPH particles into the orbital plane are shown at two different times. The units are such that $G = M = R = 1$, where M and R are the mass and radius of a neutron star. The orbital rotation is counterclockwise.

During the dynamical evolution, about 20% of the total mass is ejected from the central object through the outer Lagrangian points of the effective potential and spirals out rapidly (Fig. 2). The spiral arms, although transient in nature, form a very extended coherent structure that can subsist for a large number of internal dynamical times. Unfortunately, the spatial (and mass) resolution of the numerical simulations is not sufficient to determine accurately the internal structure and dynamical evolution of the spiral arms. Fragmentation is expected since they are strongly self-gravitating. This may indeed be visible in the outer parts of the spiral arms at late times in the simulations (see Fig. 2b), but both the size of the fragments and the thickness of the arms elsewhere are at the limit of the spatial resolution. Therefore, we now turn instead to a simple qualitative analysis of the dynamical evolution of the ejected material.

3.2 Qualitative Analysis of Spiral Arm Fragmentation

Self-gravitating fluid jets and cylinders are subject to “sausage” instabilities (also called “varicose” instabilities, cf. Chandrasekhar 1961). These instabilities lead to fragmentation into self-gravitating lumps of fluid, with the typical diameter of each lump comparable to the wavelength of the fastest growing mode, $\lambda_f = 2\pi R/0.580$, where R is the radius of the cross-section. Since both the total length and the typical curvature radius of a spiral arm are much larger than the arm’s diameter, we can treat the arms approximately as long, thin cylinders of fluid.

The numerical simulations indicate that about 20% of the total mass is ejected into the spiral arms. Each arm may then contain a mass $M_u \sim 0.3M_\odot$. The typical radius of the arm’s cross-section is $R_u \simeq 2\text{--}3$ km, while its total length is $L_u \sim 200\text{--}300$ km. The typical mean density in the arms is therefore $\rho_u \sim 10^{14} \text{ g cm}^{-3}$. We can now estimate the typical number of fragments that should form. The most unstable wavelength is $\lambda_f \sim 20$ km, so each arm should fragment into $N_f \sim L_u/\lambda_f \sim 10$ lumps, each containing a mass $M_f \sim 0.03M_\odot$. The tidal field of the central object, of mass $M_c \simeq 2.2M_\odot$, becomes important within $r_{\text{tidal}} \simeq R_u(M_c/M_f)^{1/3} \sim 10$ km. Most of the fragments form well outside of this distance

and should therefore be strongly self-gravitating.

The characteristic time for break-up is $\tau_f \simeq 4 \times (4\pi G \rho_a)^{-1/2} \sim 1$ ms (Chandrasekhar 1961). This is shorter than the β -decay time scale $\tau_\beta \simeq 20 \Delta^{-4} \mu_{e,100}^{-2}$ ms, where Δ in MeV measures the deviation of matter from β -equilibrium and $\mu_{e,100}$ is the electron chemical potential in units of 100 MeV. Thus matter in the spiral arms fragments *before* becoming unstable to β -decay. The resulting self-gravitating lumps have masses $\ll M_{\min}$ and are therefore highly unstable. Explosions should occur, similar to the one calculated in §2. We estimate below the energy release, following Colpi et al. (1989, 1993).

3.3 Relevance to Gamma-Ray Bursts

Each unstable fragment of mass $M_f \sim 0.03 M_\odot$ should release $\sim 10^{49}$ erg in antineutrinos with mean $\bar{\nu}$ -energy ~ 5 MeV. At the onset of explosion, the luminosity $L_\nu \sim N_f \times 10^{50} - 10^{52}$ erg s $^{-1}$. The thermal energy content resulting from β -decays and fissions in each fragment is $\simeq \epsilon_B (M_f/m_B) \sim 10^{49}$ erg and is available for photon emission. The estimate of the photon energy release is, however, quite uncertain. If the length scale of temperature gradients at the surface of each expanding fragment is comparable to the photon mean free path, the photon luminosity can be as large as $L_{ph} \sim 2\pi R_a \lambda_f \sigma T^4 \sim 10^{48}$ erg s $^{-1}$ for $T = 10^{10}$ K. X -rays and γ -rays would be produced with total luminosity $N_f L_{ph} \sim 10^{49}$ erg s $^{-1}$. Photon absorption could reduce this estimate by several orders of magnitude, however (Colpi et al. 1991). The kinetic energy of the exploding debris, $E_k \sim 10^{49}$ erg is not large enough for the material to climb out the gravitational potential of the central merger.

The time structure of the antineutrino and photon bursts depends on two relevant time scales: the fragmentation time $\tau_f \sim 1$ ms (which is also roughly equal to the typical time for a fragment to cross the line of sight), and the explosion time, comparable to τ_β . This time can vary between a millisecond and a few seconds, depending on the type of initial evolution out of β -equilibrium. The detailed hydrodynamics of the break-up process will determine the exact distribution of explosion times, as well as the total duration of the burst.

Conclusions

If they are cosmological in origin, γ -ray bursts require a photon energy release $\sim 10^{51}$ erg. This simple energy requirement is probably *not* satisfied by the mechanism discussed above. Under rather optimistic assumptions, we estimate that the exploding fragments carry out at most a total energy $\sim 10^{50}$ erg. Nevertheless, if γ -ray bursts are indeed produced by coalescing neutron star binaries, the emission from these exploding fragments may contribute to the total luminosity and affect the spread and shape of the burst profile.

References

- Chandrasekhar, S. 1961, *Hydrodynamic and Hydromagnetic Stability* (Oxford: Oxford University Press), Chap. XII
 Blinnikov et al. 1984, *Soviet Astron. Lett.*, **10**, 177
 Blinnikov et al. 1990, *Soviet Astron.*, **34**(6), 595
 Bildsten, L., & Cutler, C. 1992, *ApJ*, **400**, 175
 Clark, J. P. A., & Eardley, D. M. 1977, *ApJ*, **215**, 311
 Colpi, M., Shapiro, S. L., & Teukolsky, S. A. 1989, *ApJ*, **339**, 318
 Colpi, M., Shapiro, S. L., & Teukolsky, S. A. 1991, *ApJ*, **369**, 422
 Colpi, M., Shapiro, S. L., & Teukolsky, S. A. 1993, *ApJ*, **414**, 717
 Kochanek, C. S. 1992, *ApJ*, **398**, 247
 Lai, D., Rasio, F. A., & Shapiro, S. L. 1993, *ApJ*, **406**, L63
 Lai, D., Rasio, F. A., & Shapiro, S. L. 1994, *ApJ*, in press (Jan. 10)
 Narayan, R., Paczyński, B., & Piran, T. 1992, *ApJ*, **395**, L83
 Rasio, F. A., & Shapiro, S. L. 1992, *ApJ*, **401**, 226
 Rasio, F. A., & Shapiro, S. L. 1994, *ApJ*, submitted